HHS Public Access

Author manuscript

Brain Stimul. Author manuscript; available in PMC 2023 May 10.

Published in final edited form as:

Brain Stimul. 2023 ; 16(1): 56–67. doi:10.1016/j.brs.2022.12.011.

Robust enhancement of motor sequence learning with 4 mA transcranial electric stimulation

Gavin Hsu[a,*], **A. Duke Shereen**[b], **Leonardo G. Cohen**[c], **Lucas C. Parra**[a]

[a]Department of Biomedical Engineering, The City College of New York, The City University of New York, New York, NY, USA

[b]Advanced Science Research Center at the Graduate Center of the City University of New York, USA

[c]Human Cortical Physiology and Neurorehabilitation Section, National Institute of Neurological Disorders and Stroke, National Institutes of Health, Bethesda, MD, USA

Abstract

Background and objectives: Motor learning experiments with transcranial direct current stimulation (tDCS) at 2 mA have produced mixed results. We hypothesize that tDCS boosts motor learning provided sufficiently high field intensity on the motor cortex.

Methods: In a single-blinded design, 108 healthy participants received either anodal (N = 36) or cathodal (N = 36) tDCS at 4 mA total, or no stimulation (N = 36) while they practiced a 12-min sequence learning task. Anodal stimulation was delivered across four electrode pairs (1 mA each), with anodes above the right parietal lobe and cathodes above the right frontal lobe. Cathodal stimulation, with reversed polarities, served as an active control for sensation, while the no-stimulation condition established baseline performance. fMRI-localized targets on the primary motor cortex in 10 subjects were used in current flow models to optimize electrode placement for maximal field intensity. A single electrode montage was then selected for all participants.

Results: We found a significant difference in performance with anodal vs. cathodal stimulation (Cohen's d = 0.71) and vs. no stimulation (d = 0.56). This effect persisted for at least 1 h, and subsequent learning for a new sequence and the opposite hand also improved. Sensation ratings were comparable in the active groups and did not exceed moderate levels. Current flow models suggest the new electrode montage can achieve stronger motor cortex polarization than alternative montages.

*Corresponding author. ghsu@ccny.cuny.edu (G. Hsu).

Declaration of competing interest

The authors declare the following financial interests/personal relationships which may be considered as potential competing interests: LP is listed as inventor in patents owned by CCNY, and has shares in Soterix Medical Inc.

Appendix A. Supplementary data

Supplementary data to this article can be found online at https://doi.org/10.1016/j.brs.2022.12.011.

CRediT author statement

Gavin Hsu: Software, Methodology, Formal analysis, Investigation, Writing - Original Draft, Visualization. A. Duke Shereen: Methodology, Formal analysis, Investigation, Resources, Funding Acquisition. Leonardo G. Cohen: Conceptualization, Methodology. Lucas C. Parra: Conceptualization, Methodology, Supervision, Writing - Review & Editing, Funding Acquisition.

Conclusion: The present paradigm shows a medium to large effect size and is well-tolerated. It may serve as a go-to experiment for future studies on motor learning and tDCS.

Keywords

Transcranial direct current stimulation; Motor learning; Safety; Sensation; Motor cortex

1. Introduction

Prior human behavioral studies have attempted to enhance motor learning through transcranial direct current stimulation (tDCS). Motor learning has been shown in both human and animal experiments to induce synaptic plasticity in the primary motor cortex (M1) [1–4], and became a topic of early tDCS research interest [5]. These studies were based on the finding that tDCS can induce a robust change in excitability in M1 [6,7], which undergoes changes in activity and excitability during motor sequence learning [3,8–18]. As such, anodal tDCS over M1 was expected to depolarize the target membrane and facilitate learning. While the initial study by Nitche et al. (2003) saw an improvement in performance [5], the ensuing literature has seen mixed results [19]. Several studies reported that concurrent anodal stimulation over M1 or the cerebellum enhances motor sequence learning [20–24]. Others found that M1 stimulation did not affect learning, even though excitability was increased [25]. Later studies saw no effect of cerebellar tDCS on either learning performance, or neuronal activity recorded with functional magnetic resonance imaging (fMRI) [26,27]. Potential issues listed in the review by Buch et al. (2017) include a lack of reproducibility and standardization of protocols, as well as an incomplete understanding of inter-subject variability in tDCS effects [19]. Sample size in tDCS studies has also been brought up as a point of concern [28]. In sum, we are still lacking a dependable behavioral method for assessing efficacy of tDCS in modulating motor learning.

To address this, we sought to develop a novel paradigm based on our underlying theory of the effects of tDCS on synaptic efficacy. It is thought that tDCS enhances learning by modulating synaptic efficacy [29], and a key ingredient of synaptic plasticity is membrane polarization, which is affected by direct current stimulation via direct polarization and modulated firing [30,31]. Thus, applying stimulation concurrently to plasticity induction can boost learning. The importance of concurrent stimulation has already been demonstrated in the context of motor sequence learning [21]. Induced electric field intensities are likely another important factor in tDCS effects. Typical current intensities up to 2 mA [19] are estimated to induce less than 1 V/mv [32], well below values used *in vitro* to demonstrate effects on plasticity [30,31,33–36]. We have demonstrated *in vitro* that synaptic plasticity effects increase with stimulation intensity [30,35]. Such a relationship between plasticity effects and dosage has not been established conclusively in human studies [37–40], although motor learning performance has been shown to improve when using 4 mA [41]. Most tDCS experiments avoid intensities above 2 mA due to increased discomfort and difficulty in blinding, and the effects and dose response of higher-intensity tDCS therefore remain largely unexplored. We can expect that stimulation along the somatodendritic axis would maximally polarize neurons [42]. Since the somatodendritic axis of pyramidal neurons is

typically oriented normal to the cortical surface [43], the cortical surface may serve as an approximation of pyramidal neuron orientation [44]. Currents that are tangential to the scalp are therefore likely to be more effective when targeting M1 [44,45]. Yet, most studies on motor learning use the M1-SO (M1-supraorbital) montage with predominantly radial currents [19]. Finally, our theory predicts that stimulation effects should be specific to the synaptic connections undergoing plasticity, which we also confirmed *in vitro* [30]. This would suggest that behavioral effects of tDCS should be specific to the learned task.

Here we took a systematic approach to increase effective intensity on target by applying state-of-the-art targeting techniques to maximize field intensity orthogonal to cortical surface, which is the predominant orientation of pyramidal neurons [43]. The timing- and task-specific effects of this stimulation method were tested on motor sequence learning. We sought to avoid excessive discomfort by spreading out currents on the scalp [46–48], across four pairs of 12 mm diameter high-definition electrodes, each passing 1 mA for a total current of 4 mA fMRI was used to localize an active target region for motor learning in a small sample of 10 subjects. Then, through current flow modeling we optimized placement of the eight electrodes to maximize polarizing intensity, as opposed to focality [45] on the target in each head. From these individualized layouts a generalized montage was derived. Our models predicted that this electrode montage would confer stronger membrane polarization than commonly used layouts. To match the inevitable sensation effects at 4 mA, we compared anodal vs. cathodal stimulation in two different cohorts. A third, no-stimulation control group was included to control for the effects of cathodal stimulation on motor learning [21]. Across these three conditions we expected a monotonic effect on performance. We compared the behavioral effects under these conditions through a well-established sequential “finger tapping task” (FTT) that has been used to study procedural and motor skill learning [8,49–51] and applied in tES studies [22,27]. A sample size of N = 36 per group was selected, based on a power analysis of a previous study with the same task [49]. We hypothesized that 4 mA tDCS can enhance concurrent motor sequence learning with medium to large effect sizes (H1). Furthermore, we expected this boosting effect to last over time (H2). Based on our prior *in vitro* DCS work, we hypothesized that the lasting tDCS effect is specific to the hemisphere paired with stimulation (H3) and specific to the sequence paired with stimulation (H4).

2. Methods

2.1. Target location

Stimulation target locations were determined based on the fMRI activation in a finger tapping task that is closely related to the FTT. We did this in a smaller imaging cohort (10 healthy adults, 2 female, 8 male, age range = 18–55 years, mean ± SD = 24.2 ± 6.12 years). We also obtained T1 images for the purpose of current flow modeling and montage optimization (see below). All participants provided written informed consent to participate in this research, under approval of the City University of New York Institutional Review Board (IRB). Exclusion criteria for potential participants included any history of neurological or psychiatric disorders, traumatic brain injury, disabilities in the upper extremities, severe visual impairment, and any MRI contraindication.

Participants were scanned in a Siemens 3 T Prisma MRI (Siemens, Munich, Germany) at the City University of New York's Advanced Science Research Center using a 32 channel head coil receiver. The data for each participant consisted of a sagittal threedimensional T1-weighted magnetization-prepared rapid gradient echo (MPRAGE) anatomical scan and a functional echo planar imaging scan during a hand-motor task. The anatomical scans were collected with the following parameters: 208 slices, TR/TE/TI = 2400/2.15/1000 ms, slice thickness = 1 mm, flip angle = 8°, FOV = 256 ×240, in-plane resolution = 256 × 240 mm^2, and acquisition time = 5:42 min. Task fMRI were collected using an echo-planar imaging scan: 60 interleaved axial slices, slice thickness = 2.4 mm, no slice gap, multiband factor = 6, TR/TE = 800/30 ms, flip angle = 52°, FOV = 216 ×216 mm^2, in-plane resolution = 90 × 90, and acquisition time = 6:54 min. During task fMRI, participants held one 4-button response pad in each hand, with one finger on each button. Prompted by a computer monitor, the participants pressed buttons in alternating sets of 30 s on one hand at a time, alternating between hands with 30 s of rest between sets. To simulate the FTT, during each set participants pressed the buttons one at a time in sequence from the pinky toward the index finger and repeated this sequence as many times as possible during the 30 s. 10 sets were completed for each hand, for approximately 10 min total during the fMRI session. Contrasts in blood oxygenation level dependent (BOLD) signal intensity during performance of finger tapping were calculated in AFNI (Analysis of Functional NeuroImages) relative to the signals during the rest periods (separately for left and right hands). Subject level preprocessing included: slice time correction, despiking, coregistering the functional time series to a target volume and aligning the anatomical to the coregistered data, censoring data with motion greater than 1 mm from the target volume, smoothing the fMRI by applying a 5 mm Gaussian kernel to the brain extracted data, bandpass filtering between 0.01 and 0.1 Hz, and detrending the time series to correct for signal drift. To remove artifact from signal, time series data from the white matter and cerebral spinal fluid, along with 6 motion regressors from the registration were included as nuisance regressors in AFNI's '3dDeconvolve' function which modeled the data to the input stimulus (left/right/rest finger tapping blocks) and produced statistical maps of the regression beta coefficients and t-statistics for significance of the coefficients. The resulting t-statistic maps were thresholded to determine the voxels most active during sequential finger movement (Fig. 1, for left hand). We focus on the left hand (right hemisphere) as the sequence learning task will target the non-dominant hand in right-handed participants. Cortical parcellation was performed using FreeSurfer [52,53], which we used to narrow down active regions to the "hand knob" area on the precentral gyrus, and within those boundaries manually selected a single voxel with maximal or near-maximal statistical value as the target.

2.2. Electrode placement

For each participant in the imaging cohort (N = 10), we first determined the desired field orientation, designated as the orthogonal unit vector to the cortical surface at the target. This was done by loading each anatomical image in a MATLAB (MathWorks, Natick, MA) graphical user interface (GUI) that displayed the 2-D sagittal, coronal, and axial views of the head. The GUI showed the origin of the vector at the target voxel, and the second point of the vector was selected manually. Polarity of the stimulation dictated whether the vector pointed into or out of the cortical surface. The resulting 3-D directional vector was

automatically recorded as a unit vector by the program. For reproducibility of results without the need for costly individual MRIs (given the large sample size), we sought to create a single montage that provided reasonable results for all 10 participants in the imaging cohort. We selected a common desired field orientation by averaging orientation across all 10 subjects (33° from to the anterior/posterior direction and 11.3° from the horizontal/axial plane). We then generated a current flow model using ROAST (Realistic, vOlumetric Approach to Simulate Transcranial electric stimulation) [45,54,55] in MATLAB for each of the individual T1-weighted anatomical MRIs. Individualized 4+4 HD-tDCS montages were generated using ROAST's "leadfield" and "targeting" options. The electrode locations were optimized for maximum electric field intensity at the target voxel and normal to the cortical surface. Note that maximal intensity differs from the objective of focal stimulation, which are two conflicting criteria [55]. As such, we did not expect field distributions to be focal, but rather optimal in intensity. Total current was limited to 4 mA with 1 mA per electrode pair across 4 anodes and 4 cathodes (4+4) [56] selected from candidate locations in the 10-10 international system (an example of a model in one subject is shown in Fig. 2a and b). To decide on a single generalized montage we tallied the "votes" of how often a given electrode was selected (Fig. 2c). The four locations with the most "votes" were selected for each polarity to yield the final montage (Fig. 2d). Under the anodal condition, the cathodes are in the frontal positions of F4, F2, AF4, and Fz, and the anodes are in the parietal positions of P4, CP4, CP2, and P2. Here we define "anodal" stimulation as inward current on the targeted cortical structure, and the polarity of each electrode is reversed in "cathodal" stimulation, with opposite current flow directions. A reference electrode was placed at CP3 (drawing no current). After the generalized 4+4 HD montage was selected, individual ROAST models were simulated using the same 10 MRI samples for later analysis.

2.3. Stimulation and behavioral task

2.3.1. Participants—For the motor sequence learning task 108 healthy, right-handed adults (52 female, 56 male, age range = 18–55 years, mean ± SD = 24.6 ± 6.42 years) provided written informed consent to participate in this study, under approval of the City University of New York IRB. Exclusion criteria for potential participants included left-handedness, any history of neurological or psychiatric disorders, use of medication for those disorders, traumatic brain injury, disabilities in the upper extremities, or severe visual impairment. People with very thick or braided hair and those who wore a weave or wig were not included. Musicians were also excluded from the study, including professionals and amateurs who were regularly practicing a musical instrument that involves fine sequential finger movements, such as piano, guitar, violin, and trumpet, and those who had recent or extensive prior experience with such instruments but have since stopped playing. Most but not all subjects were naive to tDCS and electrical stimulation. All subjects completed the full session of experimental procedures, even though they were allowed to withdraw due to discomfort at any point during the procedure.

2.3.2. Experimental design—In a single-blind design, participants were randomly assigned to receive either anodal or cathodal stimulation (polarities as defined above; N = 36 per group). Anodal stimulation serves as the active, excitatory condition. Cathodal stimulation serves as the active control condition because at 4 mA the sensation is noticeable

and cannot be reasonably shammed (see Fig. S7). To establish an unstimulated control level of learning, we subsequently tested a control group where all subjects obtained no stimulation (N = 36). However, in order to simulate the stimulation environment as closely as possible, participants in the no-stimulation control group underwent the same procedures as the other two groups, including wearing a cap and having gel applied to the scalp, and they were informed that they may be stimulated. Sample size for each group was determined a priori based on performance data collected by Bönstrup et al. [49] in G*Power 1.3 [57]. Predicting a 30% increase in performance with stimulation, the effect size Cohen's d was determined to be approximately 0.64, and with an error probability of 5% and expected 85% power on a one-sided, two-sample *t*-test, we set the group sample size at 36.

2.3.3. Procedure—Stimulation was administered using a Soterix M×N9 HD-tES System (Soterix Medical, New York, NY) with silver/silver chloride sintered ring high-definition electrodes (Soterix Medical, New York, NY) attached to a 10-10 HD-Cap (Soterix Medical, New York, NY) at the positions determined above (Fig. 2d), with conductive gel (SignaGel, Parker Laboratories, Fairfield, NJ) applied between the scalp and electrodes. The ring electrodes have an outer radius of 6 mm, an inner radius of 2.5 mm, and a height of 1 mm. The contact area of the electrode holder base is approximately 2.7 cm^2. There is an approximately 9–10 cm distance (depending on head geometry) between the parietal electrodes and the frontal electrodes.

Participants were seated in front of a computer monitor and a keyboard with 4 adjacent keys labeled "1", "2", "3", and "4" from left to right. The FTT described here follows the procedures detailed by Bönstrup et al. [49], originally conceived by Karni et al. [8] At the beginning of each FTT section, the participants were asked to place their left hand on the labeled keys (Fig. 3a). Each iteration of the task consisted of 36 continuous trials, each 20 s long. During the first 10 s of each trial a sequence of 5 digits appeared on the monitor in a MATLAB GUI. Participants were instructed to press the keys corresponding to the numbers shown on screen in the order they appear in, from left to right, "as quickly and as accurately as possible". They were to complete the sequence as many times as possible during those 10 s, which were followed by a 10-s rest interval. The same sequence was displayed throughout all trials in one iteration of the FTT. Before the task, subjects were familiarized with the finger placement on the keyboard and the visual interface by pressing a basic, intuitive sequence of 1-2-3-4-1.

The experiment was divided into two sessions: the main task session to test hypothesis H1 and the follow-up session to test hypotheses H2–H4 (Fig. 3b). During the initial session, participants received stimulation simultaneously while they performed the FTT with sequence S1 (4-1-3-2-4) using their left hand. The stimulation intensity was ramped up over 30 s until it reached a maximum intensity of 4 mA (1 mA at each electrode), at which point the participants began the task. Like the FTT, tDCS lasted for 12 min, after which current ramped down over 30 s back to zero. A visual analog scale (Wong-Baker FACES pain scale) was administered immediately after stimulation ended. Subjects were asked to rate sensation levels from 0 to 10, 10 being the most severe, at points throughout the stimulation session: the beginning, middle, and after stimulation. Sensation quality ratings at each time

point were also collected, from the options: “No sensation”, “Tingling”, “Pricking/Stinging”, “Itching”, “Burning”, “Other”.

Between the two sessions the participants had a break of 1 h and were free to engage in any activity (typically they engaged with their book, smartphone, personal laptop, or went out to get lunch). The followup session began with a repeat of S1 as a test of lasting learning effect. Next, subjects learned sequence S2 (2-3-1-4-2) for 12 min with the same FTT, but now using the right hand. The aim here was to test if there were carry-over effects to the unstimulated hemisphere. This was then immediately followed by learning sequences S3 (3-4-2-1-3) back on the left hand again with 12 min of FTT. The aim was to test if there were carry-over effects to a new sequence in the stimulated hand. Note that neither of these follow-up learning tasks were paired with tDCS.

2.3.4. Statistical analysis—All statistical analyses were done in MATLAB. The primary measure of FTT performance is the number of fully completed sequences during each trial. Additionally, the inverse of the average time interval between keypresses within those fully correct sequences, as well as incomplete but correct sequences at the end of each trial, was taken as the tapping speed for each trial, as described by Bönstrup et al. [49] Normality of the performance metrics was assessed using the Lilliefors test, and equivalence of variances was checked using F-tests. Planned comparisons of the number of correct sequences and tapping speed between the anodal and cathodal groups were done using a two-sample *t*-test on the performance metrics averaged over the entire 12 min of the task. The same analyses were applied to test H2–H4. After the no-stimulation control was added, a fixed-effect linear model was used to test whether the number of correct sequences scales with stimulation current across all three stimulation conditions (−4 mA, 0 mA, +4 mA) as post hoc analysis, in addition to two-sample t-tests between the anodal and no-stimulation groups. Bayes Factor analysis was used to quantify the favorability of the null hypothesis that two values are equal, as described by Rouder et al. [58]. Nonparametric tests were used where assumptions of normality are violated. This was the case for the data in Fig. 5b and c and S3, where the Mann-Whitney *U* test was used for comparisons between the anodal and cathodal groups, and the Kruskal-Wallis test was used to test for effects of polarity and task condition.

2.3.5. Current flow modeling—Further analysis of current flow models was performed to directly compare the estimated efficacy of the 4+4 montage against existing setups. The first is M1-SO, which has been commonly used since the earliest tDCS motor learning study [5,19,59]. The other is a common 4+1 high-definition montage, intended for focal stimulation [60]. Simulations were done using the same 10 head MRIs from the imaging cohort used for montage selection. Three separate models were generated per head, one for each montage passing 4 mA total: 1) generalized 4+4 as determined above, with 1 mA per electrode pair; 2) M1-SO with 50 × 70 × 3 mm sponge electrodes, anode over C4 delivering 4 mA and cathode over Fp1 drawing 4 mA; and 3) 4+1 with high-definition electrodes, anode over C4 delivering 4 mA and cathodes over F4, Cz, P4, and T8 drawing 1 mA each. High-definition electrodes were modeled as 9.3 mm radius discs to approximate the surface area of the gel and scalp interface. The MRI were segmented as a part of the ROAST

pipeline, using SPM12 (The Wellcome Center for Human Neuroimaging, London, UK). Estimated electric field intensity was measured in three ways from the gray matter volume: 1) as the 99th percentile electric field magnitude across the whole brain; 2) 99th percentile electric field magnitude within a 1 cm radius sphere around the target voxel; and 3) the scalar projection of the electric field vector at the target voxel onto the normal vector of the cortical surface. Paired t-tests were used to compare these results across the 4+4 and M1-SO montages.

3. Results

3.1. Anodal stimulation improves motor sequence learning

To test H1, the primary outcome measure was the number of correct sequences completed across all trials with concurrent stimulation. The number of correct sequences combines speed and accuracy, and is therefore less susceptible to individual variations in the speed-accuracy tradeoff. The learning trajectory over the 36 trials is shown in Fig. 4a. By averaging across all trials we capture early learning gains as well as late saturation of performance. The average number of correct sequences during concurrent stimulation in the anodal group was significantly higher than that of the cathodal group (Fig. 4a; Cohen's d = 0.71, t (70) = 3.0, $p = 4.3 \times 10^{-3}$, planned comparison). Tapping speed was also significantly higher in the anodal group during stimulation compared to the cathodal group (Fig. 4b; Cohen's d = 0.61, t (70) = 2.5, p = 0.014). Thus, the subjects in the anodal group not only completed the sequence correctly more times within the learning session, but also completed each sequence more quickly.

3.2. Learning gains outlasts stimulation period for at least 1 h

The effect of polarity on performance persisted 1 h after stimulation ended, in agreement with H2 (Fig. 5a). The anodal group continued to complete S1 more times than the cathodal group (t (70) = 3.1, $p = 2.6 \times 10^{-3}$, Fig. 5a), but not more quickly (t (70) = 1.7, p = 0.086, Fig. S1a).

3.3. Learning gains extends to unstimulated motor sequence and unstimulated hand

Learning gains after stimulation were not specific to the stimulated hemisphere or sequence, contrary to H3 and H4. Difference between the anodal and cathodal groups carried over to learning with the right hand starting 72 min after stimulation (Fig. 5b). There was a significant difference in the number of correct sequences (U = 915, $p = 2.7 \times 10^{-3}$, Fig. 5b) and a trend for tapping speed (t (70) = 1.9, p = 0.064, Fig. S1b). We consider the right hand as unstimulated, as field magnitudes on its motor cortex representation are negligible.

There was also a significant difference in learning of a new sequence S3 on the left hand between anodal and cathodal group 84 min after stimulation (Fig. 5c). The gain manifested in both number of correct sequences (U = 927, $p = 1.7 \times 10^{-3}$) and tapping speed (t (70) = 2.3, p = 0.024, Fig. S1c).

3.4. Anodal stimulation provided a net gain in performance over no stimulation

The follow-up experiment on a third cohort tested a no-stimulation control group (Fig. 6). The goal for this follow-up experiment was to test whether anodal stimulation improves performance over doing nothing at all, while acknowledging that sensation clearly differs to the active anodal and cathodal conditions. A linear fixed effect model including this follow up experiment shows that there is a monotonic effect of stimulation current (cathodal, control, anodal) on the number of correct sequences with concurrent stimulation ($F(1) = 8.5$, $p = 4.4 \times 10^{-3}$). This is also true for the followup tasks: $F(1) = 9.0$, $p = 3.4 \times 10^{-3}$ (1-h followup); $F(1) = 10$, $p = 1.5 \times 10^{-3}$ (other hand); $F(1) = 12$, $p = 9.6 \times 10^{-4}$ (other sequence). Post hoc analysis finds that the group with anodal stimulation outperformed the control group in terms of correct sequences (Cohen's $d = 0.56$, $t(70) = 2.3$, $p = 0.023$, planned comparison for the follow-up experiment). Tapping speed in the anodal group during stimulation was numerically higher than the control group (Fig. S2, $t(70) = 1.8$, $p = 0.071$). Thus, it appears that anodal stimulation boosts learning not just in contrast to cathodal stimulation but in absolute terms. In general, and as expected, the no-stimulation condition falls between the cathodal and anodal condition. The difference between the cathodal and no-stimulation conditions was not significant in either the number of correct sequences ($t(70) = 0.59$, $p = 0.56$) or the tapping speed ($t(70) = 0.48$, $p = 0.63$). Bayes factor analysis provides moderate evidence in favor of no difference between cathodal stimulation and control in the number of correct sequences ($BF01 = 3.5$) and in tapping speed ($BF01 = 3.7$).

3.5. Learning gains improved initial performance in new learning task

Thus far we have analyzed performance averaged over the entire 12 min of the training period, and not distinguishing gains that carry-over to initial performance vs. additional gains in learning of a new sequence. We therefore test if the carry-over effects are already present at the beginning of the follow-up tests (Fig. S3). To test this we performed separate Kruskal-Wallis tests on initial performance with factors of conditions (Lasting Effect, Other Hand, Other Sequence) and polarity (anodal, cathodal). We find that the initial number of correct sequences is affected by polarity ($H(1) = 4.4$, $p = 0.035$) and by task condition ($H(1) = 110$, $p = 1.6 \times 10^{-24}$). A two-way ANOVA suggests that there is no interaction with task condition ($F(2) = 0.15$, $p = 0.86$), but these data violate the assumption of normality. This suggests a nonspecific carry-over effect on initial performance. Note that initial performance in the first trial of the entire experiment differed in speed (Fig. S4) but not correct sequences ($U = 1.5 \times 10^{-3}$, $p = 0.74$, $BF01 = 4.12$ in favor of null hypothesis), nor can the difference in speed predict the final outcomes (see Fig. S3–S6 for more details). This suggests that the observed polarity effects are not the results of an inhomogeneous sample of participants.

3.6. Sensation of 4 mA is tolerable and well matched with active control

The post-stimulation questionnaire records at most, moderate sensation levels at the beginning of the stimulation (Fig. 7). Sensation decreases afterwards, subsiding to very mild levels by the end of the trial. Bayes Factor analysis shows that there were no significant differences in sensation ratings between the anodal and cathodal groups ($BF01 = 2.59$ in

favor of no differences at the beginning of the trial), suggesting that the boost in learning seen in the anodal group is not the result of differing sensation. This is further supported by the lack of a performance difference between the cathodal and no-stimulation groups, despite a large difference in sensation.

3.7. Estimated field magnitudes and safety implications of the 4+4 configuration

We calculated estimated field magnitudes using ROAST [54] for the generalized 4+4 electrode montage as well as the M1-SO and 4+1 high-definition montages, with each delivering 4 mA total (see Methods). As expected, a qualitative comparison of the field profiles (Fig. 8a) finds that the 4+1 configuration is more focal [45], while the 4+4 and M1-SO profiles are more diffuse. Paired t-tests predict that electric field intensity under 4+4 is significantly stronger than that under M1-SO (Fig. 8b) in gray matter across the whole brain ($t(9) = 4.7$, $p = 1.2 \times 10^{-3}$), within 1 cm of the target voxel ($t(9) = 2.6$, $p = 0.029$), and normal to the cortical surface at the target voxel ($t(9) = 9.5$, $p = 5.5 \times 10^{-6}$). Likewise, the estimated field intensity under 4+4 is stronger in all three respective measures than under 4+1 ($t(9) = 5.5$, $p = 4.0 \times 10^{-4}$; $t(9) = 4.1$, $p = 2.7 \times 10^{-3}$; $t(9) = 8.8$, $p = 9.8 \times 10^{-6}$). The last of the three is the relevant quantity in the context of our hypothesis on membrane polarization. When comparing the generalized 4+4 montage delivering 4 mA with the conventional M1-SO montage delivering 2 mA, we expect polarizing field magnitude to increase by a factor of 4 (0.47 vs 0.10 V/m).

Aside from increasing field magnitudes, the new montage is intended to reduce current density on the scalp in order to minimize skin sensation. The highest current densities on the scalp layer are 4.1 ± 0.17 A/m^2, 4.6 ± 0.27 A/m^2, and 11 ± 0.29 A/m^2 for the three configurations respectively (4+4, M1-SO, and 4+1, Fig. 8c). These values with the proposed montage at 4 mA are at least an order of magnitude below the safety threshold of preclinical studies [61].

4. Discussion

We find that anodal stimulation with inward current flow on M1 improves concurrent motor sequence learning with a medium to large effect size of 0.7 over cathodal stimulation with outward current flow. This effect outlasts the period of stimulation by at least 1 h. The active control condition ruled out the possibility that this is the result of differing sensation levels. Importantly, the difference in performance appears to reflect a net performance gain with anodal stimulation over not stimulating at all. With no dropouts out of 72 subjects, we find that distributing 4 mA across 4+4 electrodes is safe and tolerable. Modeling suggests that this protocol can achieve stronger field magnitudes in the “hand knob” in M1 and may prove more effective than commonly used setups in a future empirical comparison.

In raising stimulation intensity to 4 mA we were mindful of issues related to sensation, tolerability, and safety. Although previous efforts have demonstrated that 4 mA is generally well tolerated [41,62,63], not all studies properly accounted for differences in sensation. This is especially important at 4 mA, where sensation can no longer be shammed. Because traditional sham stimulation with ramps can provide reliably effective blinding only up to 1 mA [64–66], we used cathodal stimulation as active control with comparable sensation.

In addition, these studies delivered 4 mA across a single pair of sponge or rubber electrodes. We previously found that mitigating discomfort from direct current of more than 2 mA delivered across a single pair of electrodes can be challenging [67]. The 4+4 montage proposed here spreads out the current, passing only 1 mA per electrode. This not only reduces sensation [46], but also minimizes current density at the skin to help limit undesirable electrochemical interactions [68]. Computational model analysis suggests that the highest current density on the scalp under the 4+4 montage is less than half of that under an equivalent 4+1 montage. At 4 mA it remains one order of magnitude lower than the threshold for tissue damage (50 A/m^2 at 30 min of stimulation) [61]. Between optimization and increasing stimulation current, we estimate that the relevant field intensity here was increased four-fold over current M1-SO practice. In summary, 4 mA tDCS through a 4+4 configuration is safe, tolerable, and effective. It is nevertheless worth noting that estimated intensities remain below the levels often used *in vitro* and *in vivo* in animal experiments. We believe that with the current multi-electrode approach one may be able to further increase stimulation intensity. Although we demonstrate a positive result with 4 mA tDCS, a direct comparison with lower or higher currents would be necessary to definitively conclude whether higher currents actually confer stronger behavioral effects. Likewise, empirical comparisons against other paradigms would be required to support our estimated improvements.

These experiments are based on the general theory that tDCS modulates the excitability and synaptic plasticity occurring in M1 during motor sequence learning. However, motor learning involves in addition to M1, the cerebellum, striatum, premotor cortex, supplementary motor area (SMA) and the spinal cord [1,10,69–75]. Numerous models have proposed that functionally connected networks across the various brain regions are engaged in parallel, with varying levels of activity throughout different stages of learning [76]. Doyon et al. (2003) described the interaction of cortico-striatal and cortico-cerebellar circuits [77], both active in the fast stage of learning, engaging the cerebellum for coordination and the striatum for sequence memory. Over the course of motor sequence learning, reliance shifts from cortico-cerebellar to cortico-striatal, when adaptive functions become less essential [77]. At the same time, motor learning has been shown to correlate with changes in markers of M1 activation as measured in various neuroimaging modalities [3,8–17], so M1 appears to play a role in task representation. With successive learning sessions, M1 also undergoes structural changes reflected in gray matter volume increase [78–81]. It is possible that stimulation of M1 facilitates these changes within M1 or facilitates the broader cortico-cerebellar and cortico-striatal interactions. There is already well-established literature demonstrating tDCS effects on M1 excitability [6,7,82], although it has not been able to directly demonstrate a correlation between excitability changes and improvements in performance [25]. During motor learning, lasting changes in behavioral performance can be observed during the first seconds of learning already [83]. There is evidence of short-term consolidation within this same FTT used here [49], where a substantial portion of task performance gains happen during the short 10-s rest periods between training. Gray matter volume can change during 30–60 min of motor sequence learning, suggesting rapid plasticity [13]. It has been demonstrated that motor sequence learning for as briefly as 30 min can reduce GABA concentration in the sensorimotor cortex [14,15], and GABA

disinhibition through tDCS and other methods can facilitate plasticity [16]. BDNF secretion is also linked to motor learning and modulated by DCS [33].

Based on our previous findings with DCS, we examined the specificity of tDCS effects. We observe a carryover effect across the rest period, where learning is boosted for both a new sequence and on the opposite hand. This appears to contradict the *in vitro* DCS work in our lab on synaptic plasticity, which suggests that stimulation has to be concurrent with training and that effects are specific to the learned task (H4) [30]. Here instead we observe that learning gains extend in time to a new motor sequence practiced without concurrent stimulation, hand and note that performance was improved even at baseline for the new sequence. In the past, neural markers of plastic changes after motor learning were observed only for the trained hand [14,84], suggesting hemispheric specificity (H3). Consistent with this interpretation, we only see a follow-up gain in baseline performance on the new sequence for the stimulated hand and not for the unstimulated hand. However, given the complexity of the neural networks engaged during motor learning, the observed carryover effects may not be fully related to stimulation of M1 alone. Many motor learning studies have demonstrated that newly acquired skills can generalize to unfamiliar tasks and environments [85,86] and transfer across hemispheres [87–90]. Thus, assumptions of specificity in our hypotheses may not be fully resolved by these behavioral effects. It is possible that the stimulation's predicted lack of focality polarizes untargeted regions of the brain that contribute to learning, leading to nonspecific effects. Although we expect field intensities outside the M1 target's immediate vicinity to be low, the premotor cortex and SMA are still close enough to be stimulated. The opposite M1 is also close enough to experience a field magnitude of around 0.3 V/m, which may have facilitated intermanual transfer of learning. Because the 4+4 montage is not focal and various brain regions are involved in the task, we opted to use cathodal stimulation as an active control rather than find a neutral area to stimulate. Spatial specificity of the stimulation may be improved with montages optimized of focality or with individualized electrode montages [44], which could be tested in future studies. The application of less involved, simple finger movement tasks may help resolve effects of spatial specificity.

We draw two potential conclusions from the observation of an unspecific effect. First, the stimulation may have caused a form of meta-learning, i.e. learning in general is improved after stimulation (at least up to 84 min, when we last tested learning). Second, this meta-learning effect is not specific to the stimulated hemisphere and cannot be due to enhancement of visuomotor mapping, since that would have been specific to the trained hand. Another factor that may have led to unspecific gains is a lasting enhancement of attention. Future experiments would be needed and specifically designed to distinguish between these possibilities.

There could also be methodological explanations for the observed non-specific effect of tDCS on motor learning. For instance, despite randomization we could have had an inhomogeneous sample, i.e. the cohort of participants in the anodal group just happened to be better learners. Indeed, motor learning performance can be quite variable across subjects, as a result of long term training (e.g. in musicians) with concomitant increase in gray matter volume or density [78,91]. In addition, the experimental design does

not include a measurement of baseline learning skill prior to training. Future studies may incorporate a pre-stimulation task to help identify inhomogeneity across groups. However, a quantitative analysis of the starting performance suggests that sample differences are unlikely. Alternatively, in a single blinded experiment, the experimenter may have introduced a non-specific bias on the participants. However, given that the instructions to the participants followed a strict script, this also seems unlikely. A replication of this study on a new cohort of participants with double blinding could help address these concerns.

Nevertheless, it is safe to conclude that the observed effects were not specific to training that was concurrent with stimulation, pointing to a more general neuromodulatory mechanism. Early studies have reported non-specific lasting change in neuronal excitability in the absence of learning [6,7,92]. Later studies suggest that these lasting changes may be due to increased synaptic efficacy among other mechanisms [29]. For instance, it has often been argued that increased neuronal activity leads to an increase in BDNF synthesis and release, which could cause a lasting gain to synaptic efficacy, even during subsequent induction [33,34,93]. In contrast, the mediator of DCS effects we had previously hypothesized [30,31] is the acute modulation in membrane potential, which can only act on synaptic plasticity during concurrent stimulation. While in-vitro experimentation is needed to resolve these cellular and molecular mechanisms, ultimately we require a reliable go-to experimental protocol to test behavioral learning effects in humans. It is our hope that the protocol presented here will be independently replicated by other laboratories and thus provide a firm stepping stone on the path of progress for the science of transcranial electric stimulation. In particular, we hope this protocol can be repeated in clinical populations, such as motor stroke, to determine whether the learning gains demonstrated here in a healthy population are relevant in clinical practice.

Supplementary Material

Refer to Web version on PubMed Central for supplementary material.

Acknowledgements

We would like to thank Yu (Andy) Huang for his extensive support with using ROAST and his current-flow modeling expertise. We would also like to acknowledge the Magnetic Resonance Imaging Facility of CUNY Advanced Science Research Center for instrument use and technical assistance. This work was supported by the NIH through grants R21NS115018, R01DC018589, R01NS095123, R01NS130484.

References

[1]. Dayan E, Cohen LG. Neuroplasticity subserving motor skill learning. Neuron 2011;72(3):443–54. 10.1016/j.neuron.2011.10.008. [PubMed: 22078504]

[2]. Rioult-Pedotti MS, Friedman D, Hess G, Donoghue JP. Strengthening of horizontal cortical connections following skill learning. Nat Neurosci 1998;1(3): 230–4. 10.1038/678. [PubMed: 10195148]

[3]. Ziemann U, Iliać TV, Pauli C, Meintzschel F, Ruge D. Learning modifies subsequent induction of long-term potentiation-like and long-term depressionlike plasticity in human motor cortex. J Neurosci 2004;24(7):1666e72. 10.1523/JNEUROSCI.5016-03.2004. [PubMed: 14973238]

[4]. Monfils MH, Teskey GC. Skilled-learning-induced potentiation in rat sensorimotor cortex: a transient form of behavioural long-term potentiation. Neuroscience 2004;125(2):329–36. 10.1016/j.neuroscience.2004.01.048. [PubMed: 15062976]

[5]. Nitsche M, Schauenburg A, Lang N, et al. Facilitation of implicit motor learning by weak transcranial direct current stimulation of the primary motor cortex in the human. J Cognit Neurosci 2003;15:619–26. 10.1162/089892903321662994. [PubMed: 12803972]

[6]. Nitsche MA, Paulus W. Excitability changes induced in the human motor cortex by weak transcranial direct current stimulation. J Physiol 2000;527(3): 633–9. 10.1111/j.1469-7793.2000.t01-1-00633.x. [PubMed: 10990547]

[7]. Nitsche MA, Paulus W. Sustained excitability elevations induced by transcranial DC motor cortex stimulation in humans. Neurology 2001;57(10): 1899–901. 10.1212/WNL.57.10.1899. [PubMed: 11723286]

[8]. Karni A, Meyer G, Jezzard P, Adams MM, Turner R, Ungerleider LG. Functional MRI evidence for adult motor cortex plasticity during motor skill learning. Nature 1995;377(6545):155–8. 10.1038/377155a0. [PubMed: 7675082]

[9]. Penhune VB, Doyon J. Cerebellum and M1 interaction during early learning of timed motor sequences. Neuroimage 2005;26(3):801–12. 10.1016/j.neuroimage.2005.02.041. [PubMed: 15955490]

[10]. Penhune VB, Steele CJ. Parallel contributions of cerebellar, striatal and M1 mechanisms to motor sequence learning. Behav Brain Res 2012;226(2): 579–91. 10.1016/j.bbr.2011.09.044. [PubMed: 22004979]

[11]. Karni A, Meyer G, Rey-Hipolito C, et al. The acquisition of skilled motor performance: fast and slow experience-driven changes in primary motor cortex. Proc Natl Acad Sci USA 1998;95(3):861–8. 10.1073/pnas.95.3.861. [PubMed: 9448252]

[12]. Kawai R, Markman T, Poddar R, et al. Motor cortex is required for learning but not for executing a motor skill. Neuron 2015;86(3):800e12. 10.1016/j.neuron.2015.03.024. [PubMed: 25892304]

[13]. Olivo G, Lövdéen M, Manzouri A, et al. Estimated gray matter volume rapidly changes after a short motor task. Cerebr Cortex 2022. 10.1093/cercor/bhab488. Published online February 8, bhab488.

[14]. Floyer-Lea A, Wylezinska M, Kincses T, Matthews PM. Rapid modulation of GABA concentration in human sensorimotor cortex during motor learning. J Neurophysiol 2006;95(3):1639–44. 10.1152/jn.00346.2005. [PubMed: 16221751]

[15]. Kolasinski J, Hinson EL, Divanbeighi Zand AP, Rizov A, Emir UE, Stagg CJ. The dynamics of cortical GABA in human motor learning. J Physiol 2019;597(1): 271–82. 10.1113/JP276626. [PubMed: 30300446]

[16]. Stagg CJ, Bachtiar V, Johansen-Berg H. The role of GABA in human motor learning. Curr Biol 2011;21(6):480–4. 10.1016/j.cub.2011.01.069. [PubMed: 21376596]

[17]. Pascual-Leone A, Grafman J, Hallett M. Modulation of cortical motor output maps during development of implicit and explicit knowledge. Science 1994;263(5151):1287e9. 10.1126/science.8122113. [PubMed: 8122113]

[18]. Muellbacher W, Ziemann U, Wissel J, et al. Early consolidation in human primary motor cortex. Nature 2002;415(6872):640e4. 10.1038/nature712. [PubMed: 11807497]

[19]. Buch ER, Santarnecchi E, Antal A, et al. Effects of tDCS on motor learning and memory formation: a consensus and critical position paper. Clin Neurophysiol 2017;128(4):589–603. 10.1016/j.clinph.2017.01.004. [PubMed: 28231477]

[20]. Vines BW, Cerruti C, Schlaug G. Dual-hemisphere tDCS facilitates greater improvements for healthy subjects' non-dominant hand compared to unihemisphere stimulation. BMC Neurosci 2008;9:103. 10.1186/1471-2202-9-103. [PubMed: 18957075]

[21]. Stagg CJ, Jayaram G, Pastor D, Kincses ZT, Matthews PM, Johansen-Berg H. Polarity and timing-dependent effects of transcranial direct current stimulation in explicit motor learning. Neuropsychologia 2011;49(5):800–4. 10.1016/j.neuropsychologia.2011.02.009. [PubMed: 21335013]

[22]. Saucedo Marquez CM, Zhang X, Swinnen SP, Meesen R, Wenderoth N. Task-specific effect of transcranial direct current stimulation on motor learning. Front Hum Neurosci 2013;7. 10.3389/fnhum.2013.00333. [PubMed: 23372547]

[23]. Saimpont A, Mercier C, Malouin F, et al. Anodal transcranial direct current stimulation enhances the effects of motor imagery training in a finger tapping task. Eur J Neurosci 2016;43(1):113–9. 10.1111/ejn.13122. [PubMed: 26540137]

[24]. Liebrand M, Karabanov A, Antonenko D, et al. Beneficial effects of cerebellar tDCS on motor learning are associated with altered putamen-cerebellar connectivity: a simultaneous tDCS-fMRI study. Neuroimage 2020;223: 117363. 10.1016/j.neuroimage.2020.117363. [PubMed: 32919057]

[25]. Ambrus GG, Chaieb L, Stilling R, Rothkegel H, Antal A, Paulus W. Monitoring transcranial direct current stimulation induced changes in cortical excitability during the serial reaction time task. Neurosci Lett 2016;616:98–104. 10.1016/j.neulet.2016.01.039. [PubMed: 26826607]

[26]. Küper M, Mallick JS, Ernst T, et al. Cerebellar transcranial direct current stimulation modulates the fMRI signal in the cerebellar nuclei in a simple motor task. Brain Stimul 2019;12(5):1169–76. 10.1016/j.brs.2019.04.002. [PubMed: 30987860]

[27]. Nguemeni C, Stiehl A, Hiew S, Zeller D. No impact of cerebellar anodal transcranial direct current stimulation at three different timings on motor learning in a sequential finger-tapping task. Front Hum Neurosci 2021;15. 10.3389/fnhum.2021.631517.

[28]. Minarik T, Berger B, Althaus L, et al. The importance of sample size for reproducibility of tDCS effects. Front Hum Neurosci 2016;10:453. 10.3389/fnhum.2016.00453. [PubMed: 27679568]

[29]. Stagg CJ, Nitsche MA. Physiological basis of transcranial direct current stimulation. Neuroscientist 2011;17(1):37–53. 10.1177/1073858410386614. [PubMed: 21343407]

[30]. Kronberg G, Rahman A, Sharma M, Bikson M, Parra LC. Direct current stimulation boosts hebbian plasticity *in vitro*. Brain Stimul 2020;13(2):287–301. 10.1016/j.brs.2019.10.014. [PubMed: 31668982]

[31]. Kronberg G, Bridi M, Abel T, Bikson M, Parra LC. Direct current stimulation modulates LTP and LTD: activity dependence and dendritic effects. Brain Stimul 2017;10(1):51–8. 10.1016/j.brs.2016.10.001. [PubMed: 28104085]

[32]. Huang Y, Liu A, Lafon B, et al. Measurements and models of electric fields in the in vivo human brain during transcranial electric stimulation. Brain Stimul Basic Transl Clin Res Neuromodulation 2017;10(4):e25–6. 10.1016/j.brs.2017.04.022.

[33]. Fritsch B, Reis J, Martinowich K, et al. Direct current stimulation promotes BDNF-dependent synaptic plasticity: potential implications for motor learning. Neuron 2010;66(2):198–204. 10.1016/j.neuron.2010.03.035. [PubMed: 20434997]

[34]. Ranieri F, Podda MV, Riccardi E, et al. Modulation of LTP at rat hippocampal CA3-CA1 synapses by direct current stimulation. J Neurophysiol 2012;107(7): 1868–80. 10.1152/jn.00319.2011. [PubMed: 22236710]

[35]. Sharma M, Farahani F, Bikson M, Parra LC. Weak DCS causes a relatively strong cumulative boost of synaptic plasticity with spaced learning. Brain Stimul Basic Transl Clin Res Neuromodulation 2022;15(1):57–62. 10.1016/j.brs.2021.10.552.

[36]. Sun Y, Lipton JO, Boyle LM, et al. Direct current stimulation induces mGluR5-dependent neocortical plasticity. Ann Neurol 2016;80(2):233–46. 10.1002/ana.24708. [PubMed: 27315032]

[37]. Jamil A, Batsikadze G, Kuo HI, et al. Systematic evaluation of the impact of stimulation intensity on neuroplastic after-effects induced by transcranial direct current stimulation. J Physiol 2017;595(4):1273–88. 10.1113/JP272738. [PubMed: 27723104]

[38]. Esmaeilpour Z, Marangolo P, Hampstead BM, et al. Incomplete evidence that increasing current intensity of tDCS boosts outcomes. Brain Stimul 2018;11(2):310e21. 10.1016/j.brs.2017.12.002. [PubMed: 29258808]

[39]. Mosayebi Samani M, Agboada D, Jamil A, Kuo MF, Nitsche MA. Titrating the neuroplastic effects of cathodal transcranial direct current stimulation (tDCS) over the primary motor cortex. Cortex 2019;119:350–61. 10.1016/j.cortex.2019.04.016. [PubMed: 31195316]

[40]. Hassanzahraee M, Nitsche MA, Zoghi M, Jaberzadeh S. Determination of anodal tDCS intensity threshold for reversal of corticospinal excitability: an investigation for induction of counter-regulatory mechanisms. Sci Rep 2020;10(1):16108. 10.1038/s41598-020-72909-4. [PubMed: 32999375]

[41]. Shinde AB, Lerud KD, Munsch F, Alsop DC, Schlaug G. Effects of tDCS dose and electrode montage on regional cerebral blood flow and motor behavior. Neuroimage 2021;237:118144. 10.1016/j.neuroimage.2021.118144. [PubMed: 33991697]

[42]. Bikson M, Inoue M, Akiyama H, et al. Effects of uniform extracellular DC electric fields on excitability in rat hippocampal slices *in vitro*. J Physiol 2004;557(Pt 1):175–90. 10.1113/jphysiol.2003.055772. [PubMed: 14978199]

[43]. Radman T, Ramos RL, Brumberg JC, Bikson M. Role of cortical cell type and morphology in subthreshold and suprathreshold uniform electric field stimulation *in vitro*. Brain Stimul 2009;2(4):215–28. 10.1016/j.brs.2009.03.007.e3. [PubMed: 20161507]

[44]. Evans C, Zich C, Lee JSA, Ward N, Bestmann S. Inter-individual variability in current direction for common tDCS montages. Neuroimage 2022;260:119501. 10.1016/j.neuroimage.2022.119501. [PubMed: 35878726]

[45]. Dmochowski JP, Datta A, Bikson M, Su Y, Parra LC. Optimized multi-electrode stimulation increases focality and intensity at target. J Neural Eng 2011;8(4): 046011. 10.1088/1741-2560/8/4/046011. [PubMed: 21659696]

[46]. Borckardt JJ, Bikson M, Frohman H, et al. A pilot study of the tolerability and effects of high-definition transcranial direct current stimulation (HD-tDCS) on pain perception. J Pain 2012;13(2):112–20. 10.1016/j.jpain.2011.07.001. [PubMed: 22104190]

[47]. Reckow J, Rahman-Filipiak A, Garcia S, et al. Tolerability and blinding of 4×1 high-definition transcranial direct current stimulation (HD-tDCS) at two and three milliamps. Brain Stimul 2018;11(5):991–7. 10.1016/j.brs.2018.04.022. [PubMed: 29784589]

[48]. Gbadeyan O, Steinhauser M, McMahon K, Meinzer M. Safety, tolerability, blinding efficacy and behavioural effects of a novel MRI-compatible, high-definition tDCS set-up. Brain Stimul 2016;9(4):545–52. 10.1016/j.brs.2016.03.018. [PubMed: 27108392]

[49]. Bönstrup M, Iturrate I, Thompson R, Cruciani G, Censor N, Cohen LG. A rapid form of offline consolidation in skill learning. Curr Biol 2019;29(8):1346–51. 10.1016/j.cub.2019.02.049.e4. [PubMed: 30930043]

[50]. Walker MP, Brakefield T, Morgan A, Hobson JA, Stickgold R. Practice with sleep makes perfect: sleep-dependent motor skill learning. Neuron 2002;35(1):205–11. 10.1016/S0896-6273(02)00746-8. [PubMed: 12123620]

[51]. Censor N, Sagi D, Cohen LG. Common mechanisms of human perceptual and motor learning. Nat Rev Neurosci 2012;13(9):658–64. 10.1038/nrn3315. [PubMed: 22903222]

[52]. Desikan RS, Ségonne F, Fischl B, et al. An automated labeling system for subdividing the human cerebral cortex on MRI scans into gyral based regions of interest. Neuroimage 2006;31(3):968–80. 10.1016/j.neuroimage.2006.01.021. [PubMed: 16530430]

[53]. Fischl B, van der Kouwe A, Destrieux C, et al. Automatically parcellating the human cerebral cortex. Cerebr Cortex 2004;14(1):11–22. 10.1093/cercor/bhg087.

[54]. Huang Y, Datta A, Bikson M, Parra LC. Realistic volumetric-approach to simulate transcranial electric stimulation—ROAST—a fully automated opensource pipeline. J Neural Eng 2019;16(5):056006. 10.1088/1741-2552/ab208d. [PubMed: 31071686]

[55]. Dmochowski JP, Datta A, Huang Y, et al. Targeted transcranial direct current stimulation for rehabilitation after stroke. Neuroimage 2013;75:12e9. 10.1016/j.neuroimage.2013.02.049.

[56]. Huang Y, Datta A, Parra LC. Optimization of interferential stimulation of the human brain with electrode arrays. J Neural Eng 2020;17(3):036023. 10.1088/1741-2552/ab92b3. [PubMed: 32403096]

[57]. Faul F, Erdfelder E, Buchner A, Lang AG. Statistical power analyses using G*Power 3.1: tests for correlation and regression analyses. Behav Res Methods 2009;41(4):1149–60. 10.3758/BRM.41.4.1149. [PubMed: 19897823]

[58]. Rouder JN, Morey RD, Speckman PL, Province JM. Default Bayes factors for ANOVA designs. J Math Psychol 2012;56(5):356–74. 10.1016/j.jmp.2012.08.001.

[59]. Knotkova H, Riggs A, Berisha D, et al. Automatic M1-SO montage headgear for transcranial direct current stimulation (TDCS) suitable for home and high-throughput in-clinic applications. Neuromodulation Technol Neural Interface 2019;22(8):904–10. 10.1111/ner.12786.

[60]. Datta A, Bansal V, Diaz J, Patel J, Reato D, Bikson M. Gyri-precise head model of transcranial direct current stimulation: improved spatial focality using a ring electrode versus conventional rectangular pad. Brain Stimul 2009;2(4):201–7. 10.1016/j.brs.2009.03.005. [PubMed: 20648973]

[61]. Bikson M, Grossman P, Thomas C, et al. Safety of transcranial direct current stimulation: evidence based update 2016. Brain Stimul 2016;9(5):641–61. 10.1016/j.brs.2016.06.004. [PubMed: 27372845]

[62]. Khadka N, Borges H, Paneri B, et al. Adaptive current tDCS up to 4 mA. Brain Stimul Basic Transl Clin Res Neuromodulation 2020;13(1):69–79. 10.1016/j.brs.2019.07.027.

[63]. Workman CD, Fietsam AC, Rudroff T. Different effects of 2 mA and 4 mA transcranial direct current stimulation on muscle activity and torque in a maximal isokinetic fatigue task. Front Hum Neurosci 2020;14. 10.3389/fnhum.2020.00240. [PubMed: 32116603]

[64]. Gandiga PC, Hummel FC, Cohen LG. Transcranial DC stimulation (tDCS): a tool for double-blind sham-controlled clinical studies in brain stimulation. Clin Neurophysiol 2006;117(4):845–50. 10.1016/j.clinph.2005.12.003. [PubMed: 16427357]

[65]. O'Connell NE, Cossar J, Marston L, et al. Rethinking clinical trials of transcranial direct current stimulation: participant and assessor blinding is inadequate at intensities of 2mA. PLoS One 2012;7(10):e47514. 10.1371/journal.pone.0047514. [PubMed: 23082174]

[66]. Workman CD, Fietsam AC, Kamholz J, Rudroff T. Women report more severe sensations from 2 mA and 4 mA transcranial direct current stimulation than men. Eur J Neurosci 2021;53(8):2696–702. 10.1111/ejn.15070. [PubMed: 33259084]

[67]. Hsu G, Farahani F, Parra LC. Cutaneous sensation of electrical stimulation waveforms. Brain Stimul 2021;14(3):693–702. 10.1016/j.brs.2021.04.008. [PubMed: 33848677]

[68]. Merrill DR, Bikson M, Jefferys JGR. Electrical stimulation of excitable tissue: design of efficacious and safe protocols. J Neurosci Methods 2005;141(2): 171–98. 10.1016/j.jneumeth.2004.10.020. [PubMed: 15661300]

[69]. Seitz RJ, Roland E, Bohm C, Greitz T, Stone-Elander S. Motor learning in man: a positron emission tomographic study. Neuroreport 1990;1(1):57–60. 10.1097/00001756-199009000-00016. [PubMed: 2129858]

[70]. Doyon J, Benali H. Reorganization and plasticity in the adult brain during learning of motor skills. Curr Opin Neurobiol 2005;15(2):161–7. 10.1016/j.conb.2005.03.004. [PubMed: 15831397]

[71]. Doyon J, Bellec P, Amsel R, et al. Contributions of the basal ganglia and functionally related brain structures to motor learning. Behav Brain Res 2009;199(1):61–75. 10.1016/j.bbr.2008.11.012. [PubMed: 19061920]

[72]. Honda M, Deiber MP, Ibanez V, Pascual-Leone A, Zhuang P, Hallett M. Dynamic cortical involvement in implicit and explicit motor sequence learning. A PET study. Brain 1998;121(11):2159–73. 10.1093/brain/121.11.2159. [PubMed: 9827775]

[73]. Hikosaka O, Nakamura K, Sakai K, Nakahara H. Central mechanisms of motor skill learning. Curr Opin Neurobiol 2002;12(2):217–22. 10.1016/S0959-4388(02)00307-0. [PubMed: 12015240]

[74]. Vahdat S, Lungu O, Cohen-Adad J, Marchand-Pauvert V, Benali H, Doyon J. Simultaneous brain–cervical cord fMRI reveals intrinsic spinal cord plasticity during motor sequence learning. PLoS Biol 2015;13(6):e1002186. 10.1371/journal.pbio.1002186. [PubMed: 26125597]

[75]. Khatibi A, Vahdat S, Lungu O, et al. Brain-spinal cord interaction in long-term motor sequence learning in human: an fMRI study. Neuroimage 2022;253: 119111. 10.1016/j.neuroimage.2022.119111. [PubMed: 35331873]

[76]. Dahms C, Brodoehl S, Witte OW, Klingner CM. The importance of different learning stages for motor sequence learning after stroke. Hum Brain Mapp 2020;41(1):270–86. 10.1002/hbm.24793. [PubMed: 31520506]

[77]. Doyon J, Penhune V, Ungerleider LG. Distinct contribution of the cortico-striatal and cortico-cerebellar systems to motor skill learning. Neuropsychologia 2003;41(3):252–62. 10.1016/S0028-3932(02)00158-6. [PubMed: 12457751]

[78]. Sampaio-Baptista C, Scholz J, Jenkinson M, et al. Gray matter volume is associated with rate of subsequent skill learning after a long term training intervention. Neuroimage 2014;96:158–66. 10.1016/j.neuroimage.2014.03.056. [PubMed: 24680712]

[79]. Draganski B, Gaser C, Busch V, Schuierer G, Bogdahn U, May A. Changes in grey matter induced by training. Nature 2004;427(6972):311–2. 10.1038/427311a. [PubMed: 14737157]

[80]. Gaser C, Schlaug G. Brain structures differ between musicians and non-musicians. J Neurosci 2003;23(27):9240–5. [PubMed: 14534258]

[81]. Filippi M, Ceccarelli A, Pagani E, et al. Motor learning in healthy humans is associated to gray matter changes: a tensor-based morphometry study. PLoS One 2010;5(4):e10198. 10.1371/journal.pone.0010198. [PubMed: 20419166]

[82]. Ahn S, Fröhlich F. Pinging the brain with transcranial magnetic stimulation€ reveals cortical reactivity in time and space. Brain Stimul Basic Transl Clin Res Neuromodulation 2021;14(2):304–15. 10.1016/j.brs.2021.01.018.

[83]. Johnson BP, Tomlin KB, Censor N, Cohen LG, Westlake KP. Motor memory reactivation: Brief practice makes perfect. 2022. 10.31234/osf.io/q5y9n. Published online May 6.

[84]. Garry MI, Kamen G, Nordstrom MA. Hemispheric differences in the relationship between corticomotor excitability changes following a fine-motor task and motor learning. J Neurophysiol 2004;91(4):1570–8. 10.1152/jn.00595.2003. [PubMed: 14627660]

[85]. Sarwary AME, Stegeman DF, Selen LPJ, Medendorp WP. Generalization and transfer of contextual cues in motor learning. J Neurophysiol 2015;114(3): 1565–76. 10.1152/jn.00217.2015. [PubMed: 26156381]

[86]. Gandolfo F, Mussa-Ivaldi FA, Bizzi E. Motor learning by field approximation. Proc Natl Acad Sci USA 1996;93(9):3843–6. 10.1073/pnas.93.9.3843. [PubMed: 8632977]

[87]. Sainburg RL, Wang J. Interlimb transfer of visuomotor rotations: independence of direction and final position information. Exp Brain Res 2002;145(4): 437–47. 10.1007/s00221-002-1140-7. [PubMed: 12172655]

[88]. Carroll TJ, Poh E, de Rugy A. New visuomotor maps are immediately available to the opposite limb. J Neurophysiol 2014;111(11):2232–43. 10.1152/jn.00042.2014. [PubMed: 24598522]

[89]. Dickins DSE, Sale MV, Kamke MR. Intermanual transfer and bilateral cortical plasticity is maintained in older adults after skilled motor training with simple and complex tasks. Front Aging Neurosci 2015;7. 10.3389/fnagi.2015.00073. [PubMed: 25762930]

[90]. Dirren E, Bourgeois A, Klug J, Kleinschmidt A, van Assche M, Carrera E. The neural correlates of intermanual transfer. Neuroimage 2021;245:118657. 10.1016/j.neuroimage.2021.118657. [PubMed: 34687859]

[91]. Tomassini V, Jbabdi S, Kincses ZT, et al. Structural and functional bases for individual differences in motor learning. Hum Brain Mapp 2011;32(3): 494–508. 10.1002/hbm.21037. [PubMed: 20533562]

[92]. Bindman LJ, Lippold OC, Milne AR. Prolonged changes in excitability of pyramidal tract neurones in the cat: a post-synaptic mechanism. J Physiol 1979;286:457–77. [PubMed: 439035]

[93]. Podda MV, Cocco S, Mastrodonato A, et al. Anodal transcranial direct current stimulation boosts synaptic plasticity and memory in mice via epigenetic regulation of Bdnf expression. Sci Rep 2016;6(1):22180. 10.1038/srep22180. [PubMed: 26908001]

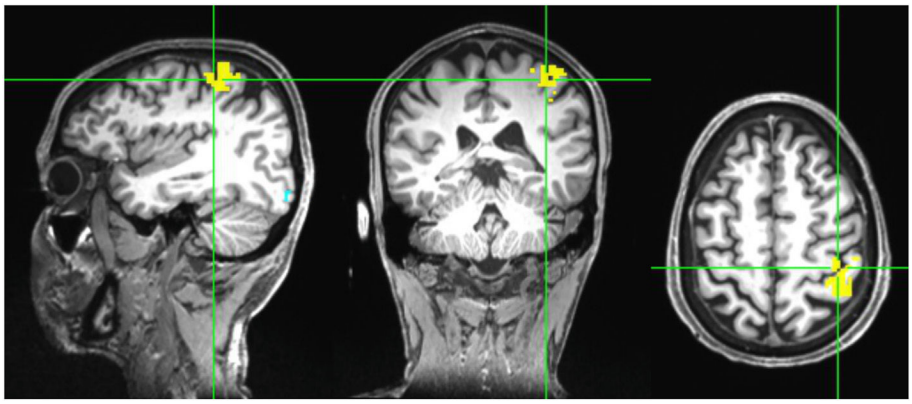

Fig. 1. Statistical map of BOLD activity during simple sequential finger tapping with left hand.
A target “hot spot” was manually selected on the cortical surface of the “hand knob” area of M1 in the precentral gyrus.

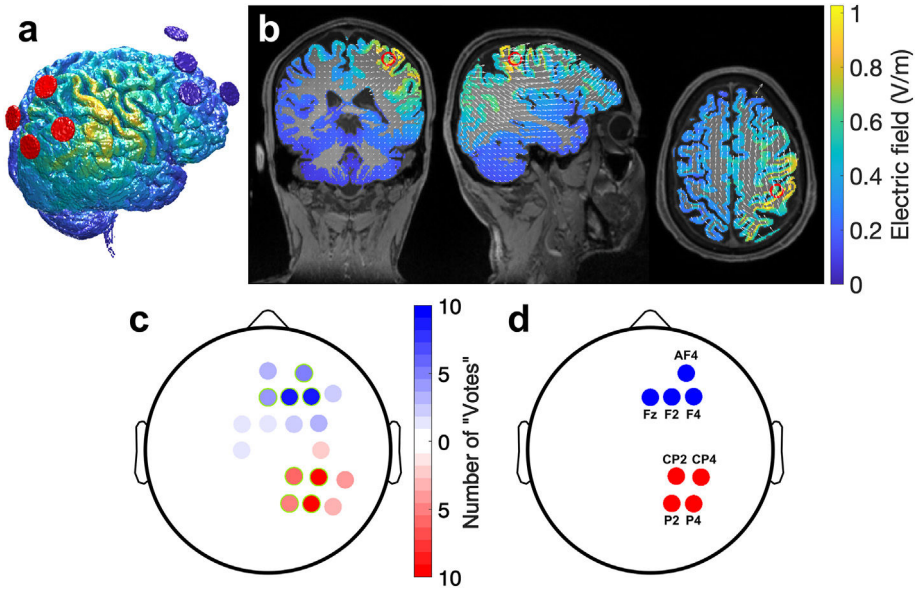

Fig. 2. Selection of electrode montage.

Electrode polarities under anodal stimulation are shown. (a) Electric field estimated for an individual subject with a 4+4 electrode montage (red and blue circles represent 4 anodes and 4 cathode, respectively). This montage was optimized to achieve maximum intensity at the voxel in the “hand knob” with the highest fMRI activation, with current flowing from posterior to anterior direction normal to the cortical surface under anodal stimulation. As expected, for maximal polarizing intensity, fields are broadly distributed. (b) 2D views of estimated electric field on gray matter resulting from stimulation for the same subject in (a). White arrows represent electric field vectors and red rings mark the manually selected “hand knob” target. (c) Tally of how often an electrode location (in the 10-10 system) was selected by the optimization routine in ROAST for the 10 individual subjects models and targets (red: anodes, blue: cathodes) (d) Locations selected (with the highest tally in panel c) for a common montage that was used for all subjects during the motor sequence learning task. Anodes (red) each inject 1 mA and cathodes (blue) each draw 1 mA for a total of 4 mA of constant current stimulation.

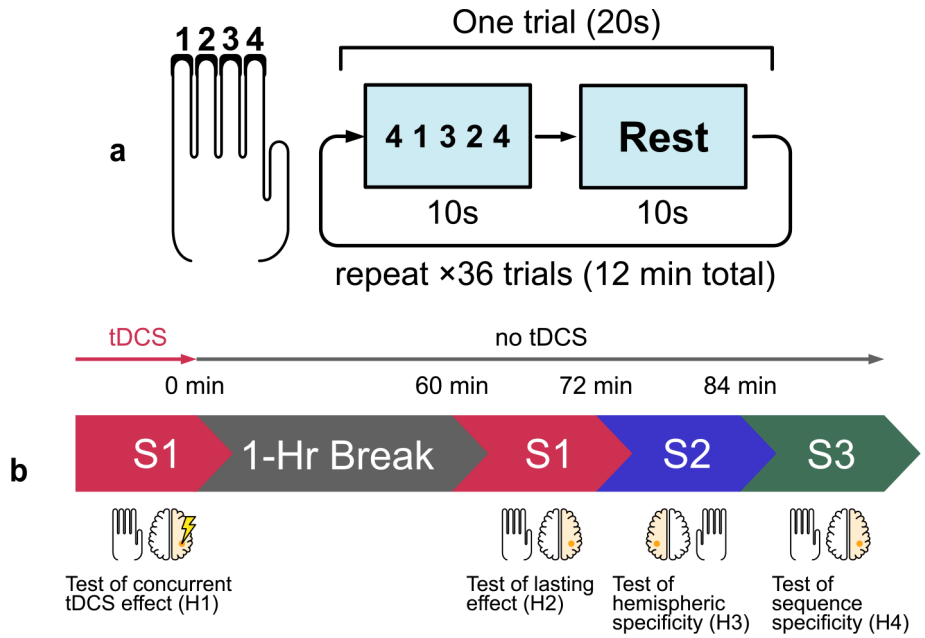

Fig. 3. Experimental protocol.

(a) Four fingers are placed on four keys labeled “1”, “2”, “3”, “4” (thumb is not used). A monitor prompts the subject to press the keys in the sequence shown. Each trial comprises a 10-s interval during which the subject repeatedly presses the sequence as fast as possible, followed by 10 s of rest. Each section contains 36 trials lasting 12 min total. (b) An initial learning section using the left (non-dominant) hand is paired with 12 min of stimulation of the contralateral hemisphere (right). This is followed by a 1-h break. The task is repeated to test for carryover effects without stimulation. Different sequences S1, S2, and S3 are used throughout different sections. S1: 4-1-3-2-4, S2: 2-3-1-4-2, S3: 3-4-2-1-3.

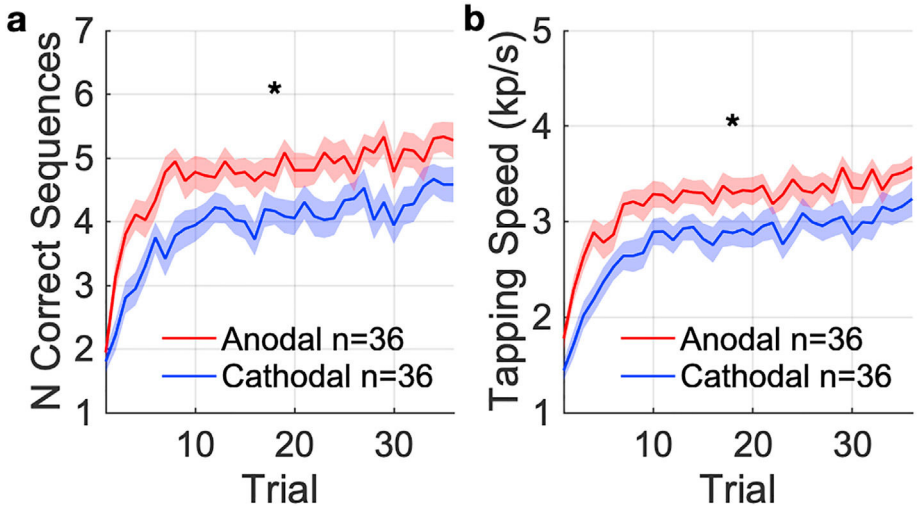

Fig. 4. Performance in the finger tapping task with concurrent tDCS targeting contralateral motor cortex.

(a) The primary outcome, measured as the number of correct sequences completed per trial (mean: solid curve, SEM: shaded area). (b) The secondary outcome, measured as the tapping speed for each trial. * indicates significant difference ($p < 0.05$) between anodal and cathodal groups in the average over all trials.

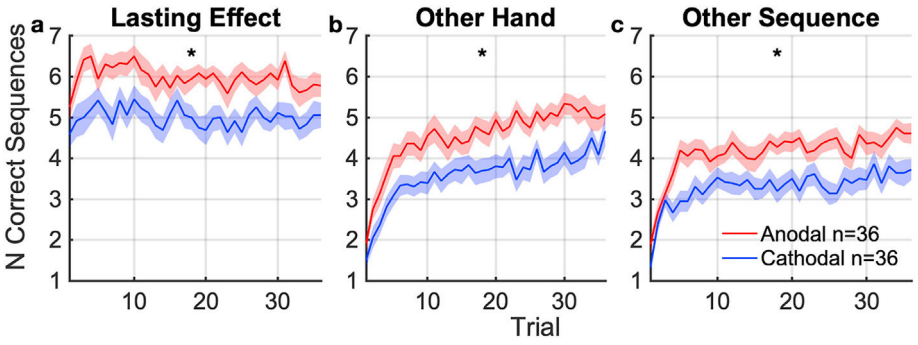

Fig. 5. Carry-over effects of stimulation on performance and learning.

Number of correct sequences completed per trial during followup tasks, averaged across subjects. (mean: solid curve, SEM: shaded area, * indicates significant difference at $p < 0.05$) between anodal and cathodal groups. (a) Performance with the same hand (left) and same sequence, tested 60 min after tDCS. This captures lasting learning effects of the targeted hemisphere and sequence. (b) Learning of a new sequence with the opposing (right) hand 72 min after tDCS. This captures lasting carry-over effects on learning to the other hand. (c) Learning of a new sequence with the same (left) hand 84 min after tDCS. This captures lasting carryover effects to learning of other sequences.

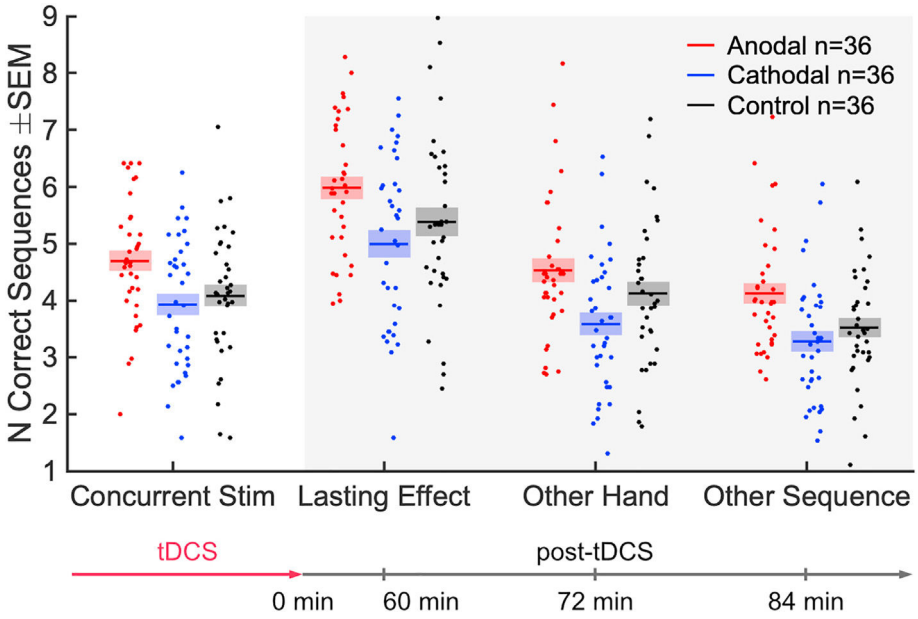

Fig. 6.

Comparison of anodal and cathodal stimulation with the follow-up control condition of no stimulation. Same data as Figs. 4a and 5, but here each point is a subject, indicating the number of correct sequences averaged over all 36 trials (mean: solid line; SEM: shaded area).

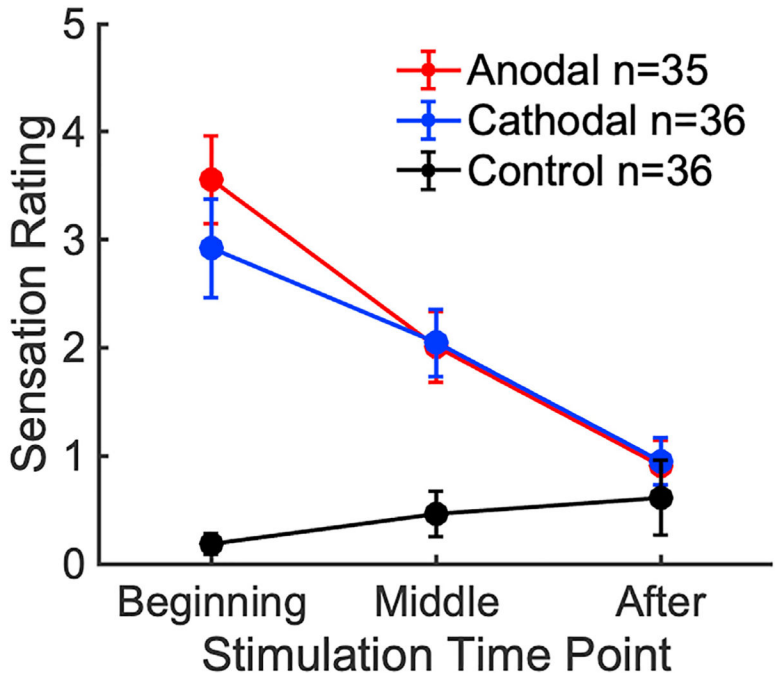

Fig. 7. Post-stimulation VAS ratings of sensation experienced throughout different points of the stimulation session.

The maximum rating participants can give is 10 (“Extreme” intensity). A rating of 5 corresponds to “Moderate” sensation. Error bars represent SEM.

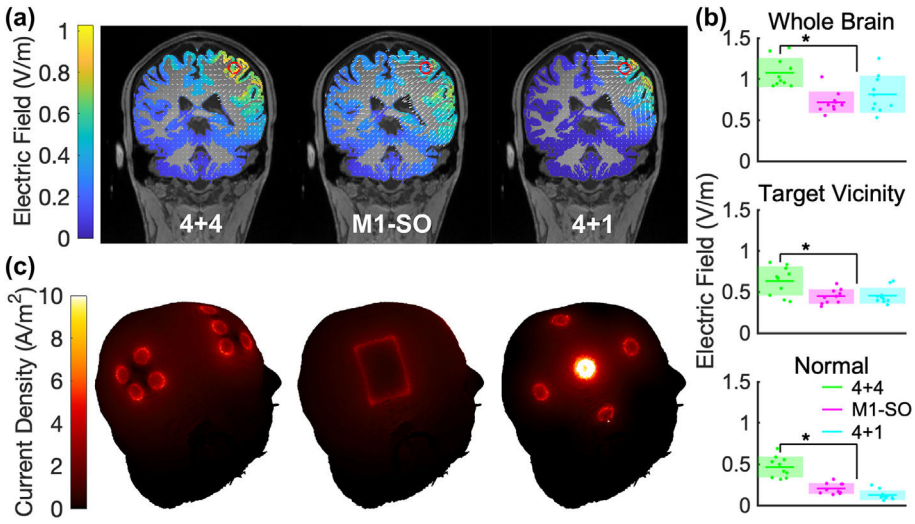

Fig. 8. Comparisons of ROAST current flow modeling results between different tDCS configurations, each delivering 4 mA total current.

Models were generated from N = 10 MRI heads. (a) Coronal views of electric field delivered to gray matter with the respective montages. The red circle marks the target and white arrows represent electric field vectors. Results from one head shown as an example. (b) Estimated electric field intensities as measured in gray matter across the whole brain, within 1 cm of the target voxel, and along the normal vector on the target voxel. Individual points represent a measurement from each of 10 heads. The colored horizontal line represents the average and the shaded area represents the standard deviation. * denotes a significant difference between 4+4 and M1-SO. (c) 3D visualizations of current density on the skin with 4+4, M1-SO, and 4+1 tDCS montages, in the same order as in (a).